JACS
JOURNAL OF THE AMERICAN CHEMICAL SOCIETY

ARTICLE

pubs.acs.org/JACS

Octadentate Cages of Tb(III) 2-Hydroxyisophthalamides: A New Standard for Luminescent Lanthanide Labels

Jide Xu,[†] Todd M. Corneillie,[†] Evan G. Moore,[†] Ga-Lai Law,[†,‡] Nathaniel G. Butlin,[‡] and Kenneth N. Raymond*[,†,‡]

[†]Department of Chemistry, University of California, Berkeley, California 94720-1460, United States

[‡]Lumiphore, Inc., 4677 Meade Street, Suite 216, Richmond, California, 94804

Supporting Information

ABSTRACT: The synthesis, structure, and photophysical properties of several Tb(III) complexes with octadentate, macrotricyclic ligands that feature a bicapped topology and 2-hydroxyisophthalamide (IAM) chelating units are reported. These Tb(III) complexes exhibit highly efficient emission ($\Phi_{total} \geq 50\%$), large extinction coefficients ($\varepsilon_{max} \geq 20{,}000\ M^{-1}\ cm^{-1}$), and long luminescence lifetimes ($\tau_{H_2O} \geq 2.45$ ms) at dilute concentrations in standard biological buffers. The structure of the methyl-protected ligand was determined by single-crystal X-ray diffraction and confirms the macrotricyclic structure of the parent ligand; the amide groups of the methyl-protected cage compound generate an anion binding cavity that complexes a chloride anion. Once the ligand is deprotected, a conformational change generates a similar cavity, formed by the phenolate and ortho amide oxygen groups that strongly bind lanthanide ions. The Tb(III) complexes thus formed display long-term stability, with little if any change in their spectral properties (including lifetime, quantum yield, and emission spectrum) over time or in different chemical environments. Procedures to prepare functionalized derivatives with terminal amine, carboxylate, and *N*-hydroxysuccinimide groups suitable for derivatization and protein bioconjugation have also been developed. These bifunctional ligands have been covalently attached to a number of different proteins, and the terbium complexes' exceptional photophysical properties are retained. These compounds establish a new aqueous stability and quantum yield standard for long-lifetime lanthanide reporters.

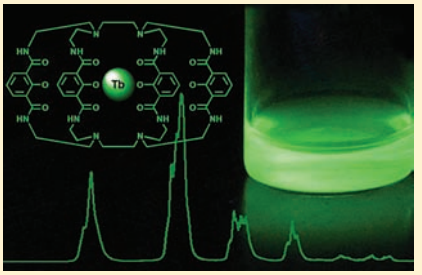

INTRODUCTION

Highly emissive luminescent lanthanide complexes with good aqueous stability are useful in a range of bioanalytical applications and particularly distinguish themselves in comparison to conventional organic fluorophores, since their long-lived luminescence facilitates their use in time-resolved homogeneous immunoassays.[1−6] While conventional organic dyes have lifetimes in the range of nanoseconds, lanthanide-based reporters can have millisecond lifetimes, enabling the time-gated removal of background autofluorescence that is otherwise problematic for fluorescence-based biological assays. In practice, pulsed excitation is used to excite an analytical sample in a complex biological matrix. Integration of the emission signal after a variable time delay allows the short-lived interfering background fluorescence and scattered excitation to dissipate while the long-lived lanthanide emission remains.

Among other approaches, a variety of bipyridine-based macrobicyclic ligands (cryptands) have been used for preparing luminescent lanthanide complexes where the bipyridine unit serves both as a chelating subunit and as an antenna chromophore.[7−11] In particular, the Eu(III) complexes of the Lehn cryptand (Figure 1, **1** and **2**) have been successfully developed for commercial immunoassays. These complexes have limited thermodynamic stability in aqueous solution but show high kinetic stability, since the macrocyclic topology provides a rigid and protective coordination environment. However, the quantum yield for these compounds and several other lanthanide reporters in wide use[12] is only on the order of 3%.[8] Although Ln(III) complexes with higher extinction coefficients and quantum yields have been described,[13,14] these do not retain their bright luminescence properties at dilute concentrations in aqueous solution.[4,13−15] Thus, there is a clear need for much brighter lanthanide reporters. For new reporters to be fully useful for biological applications, it is critical that the metal complexes exhibit high solubility, have excellent stability, and also retain the metal ion in aqueous conditions over time at physiological pH and subnanomolar concentrations.

We have previously reported a new class of luminescent lanthanide complexes with high quantum yields for multiple lanthanide ions using ligands that incorporate the 2-hydroxyisophthalamide (IAM) moiety as both an antenna chromophore and a chelating group (Figure 1, **3** and **4**).[16−20] The quantum yields reported for the Tb(III) complexes of these IAM-based ligands are over 50% in aqueous solutions at physiologically relevant pH, and visualization of their emission does not require the addition of augmenting agents such as micelles or fluoride.[21] The IAM-based structures display good thermodynamic stability

Received: August 31, 2011
Published: October 19, 2011

dx.doi.org/10.1021/ja2079898 | *J. Am. Chem. Soc.* 2011, 133, 19900–19910

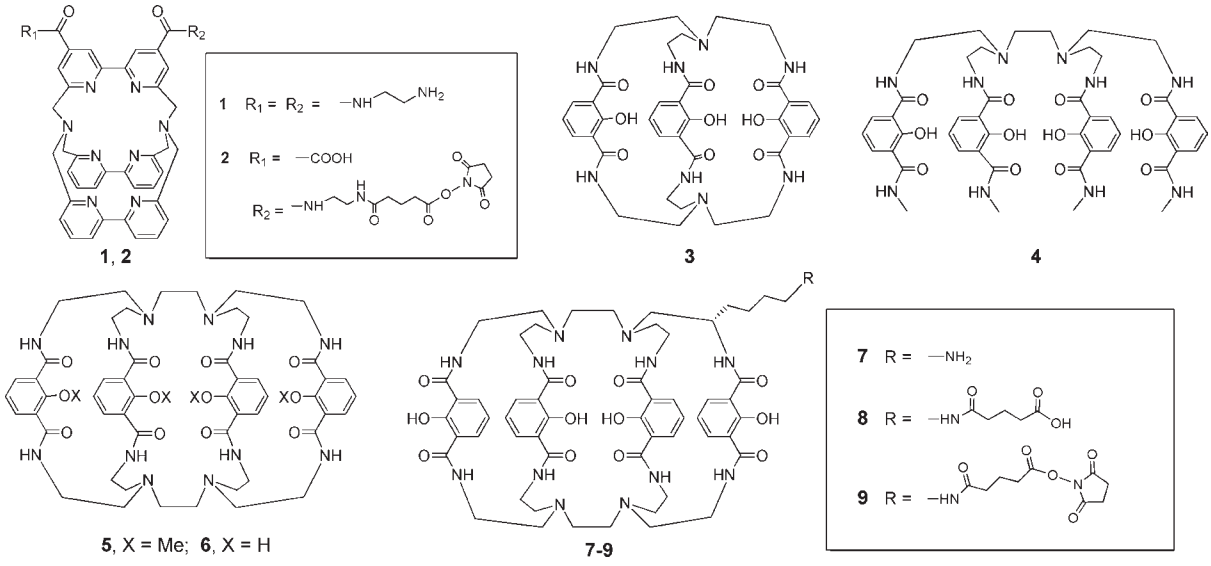

Figure 1. Chemical structures of several ligand platforms used for sensitized lanthanide luminescence. **1** was originally developed by Lehn et al.,[7] **2** is a commercial product of Cisbio.[11] **3** and **4** were developed by Raymond et al.;[16] **5**–**9** are described here.

in aqueous solution, with high molar extinction coefficients and quantum yields, and they retain all of the benefits of conventional lanthanide reporters (long fluorescence lifetimes, large effective Stokes shifts, and narrow emission lines). These properties make them exceptionally and uniquely suited to homogeneous assays. However, Tb(III) complexes of **3** and **4** have shortcomings that prevent their applicability as next-generation lanthanide reporters. For the Tb(III) complexes of **3**, which is potentially a hexadentate ligand, it was found that the metal binds with two ligands in a tetradentate manner, resulting in complexes in the form of $[Tb(\mathbf{3})_2]^-$, which is not practical for attachment as a reporter. The octadentate, acyclic 2-hydroxyisophthalamide complexing agent, H(2,2)IAM (Figure 1, **4**), forms highly luminescent complexes with Tb(III) in a phosphate buffer system with a limiting concentration of *ca.* 10 pM (1×10^{-11} M).[20] A modified version was derivatized for attachment to biomolecules, but this complex is kinetically labile in certain buffers, which results in rapid loss of the metal ion and luminescence. In addition, the conformational flexibility of this ligand allows the hydrophobic surfaces of the ligand to stick nonspecifically to protein surfaces. Thus, the general applicability of the acyclic IAM derivatives is limited.

To address these shortcomings, we have designed a macrotricyclic ligand (Figure 1, **6**) using a bicapped H(2,2) ligand topology,[22] which predisposes the metal-binding units into an environment ideal for f-element cation coordination. We have determined that the excellent thermodynamic stability demonstrated by previous IAM-based ligands is retained by the BH(2,2)IAM chelate (Figure 1, **6**), and the kinetic stability of the Ln(III) complexes is markedly improved. Also, since the IAM subunits are constrained on both ends, the nonspecific attraction to protein surfaces observed with ligand **4** has been eliminated. As a result, these macrotricyclic complexes retain their exceptional stability and extremely bright photophysical properties under a large variety of solution conditions at nanomolar concentrations and even in the presence of strongly competitive anions and cations, making these complexes fully useful under biologically relevant homogeneous assay conditions.

Furthermore, in order to provide bifunctional chelators that maintain the native properties of the Ln(III) complex following protein conjugation, another requirement is to introduce a point of attachment on the BH(2,2)IAM scaffold that is suitable for bioconjugation chemistries.[23] In this context, it is essential that the covalently conjugated reporter should not significantly alter the protein function and, conversely, that covalent attachment to the protein should not significantly alter the photophysical properties of the reporter. A single reactive functional group on the ligand is needed to preclude undesirable intra- and intermolecular cross-linking upon conjugation with biomolecules, since such cross-linking can have a dramatic and deleterious impact on the biological and immunogenic properties of the ligand–biomolecule conjugate.[24−27] Herein, we report the successful combination of these strategies to yield a family of macrotricyclic, bifunctional IAM chelators (Figure 1, **7**–**9**), and the crystal structure of the methyl protected macrotricycle Me_4BH(2,2)IAM (Figure 1, **5**). We demonstrate that the bifunctional Tb(III) complexes retain the photophysical properties of their unfunctionalized counterpart (**6**) and form highly stable and brightly luminescent compounds. Most importantly, these properties are also retained following covalent conjugation to several proteins.

RESULTS AND DISCUSSION

Synthesis of the Ligands. Entry into the chemistry of highly predisposed isophthalamide ligands was based on our bicapped tetracatecholate ligands' synthetic methodology.[22] Coupling the bis(thiazolidine-2-thione) derivative of 2-methoxyisophthalic acid[16,17] with a variety of tetrapodal amines enables the preparation of gram quantities of this class of cage ligands.

The syntheses of the IAM-based macrotricycle and macrotricyclic bifunctional chelators are outlined in Scheme 1. The preparation of the symmetrical intermediate **5** was accomplished by reaction of pentaethylene tetraamine (Penten) with the previously reported tetrathiazolidinethione **10** under high dilution conditions. Use of the thiazolidinethione leaving group, as opposed to chloride, for example, was important to minimize side

Scheme 1. Syntheses of BH(2,2)IAM and Its Monofunctionalized Derivatives[a]

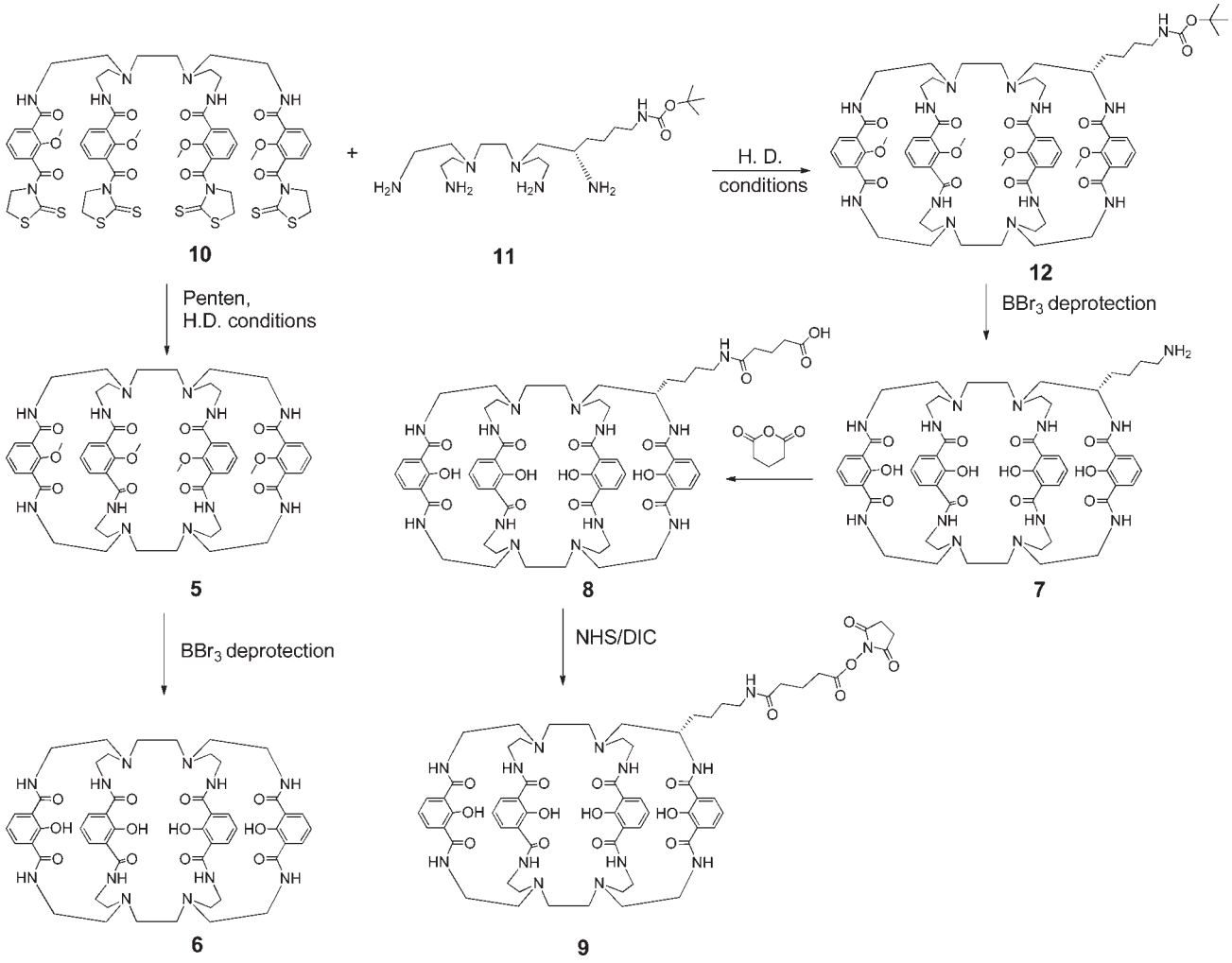

[a] Full procedures and abbreviations are given in the Experimental Section.

reactions, leading to formation of macrocycle **5** in 52% yield. Methyl group deprotection was effected using BBr_3 under standard conditions.[22]

Formation of asymmetric, bifunctional chelators required the synthesis of a protected pentaethylene tetraamine derivative containing protected side arm functionality, **11**. This was accomplished by condensing Z-protected tris(2-aminoethyl)amine with the aldehyde formed from Z- and Boc-protected lysine, followed by reaction with Z-aziridine as described.[23] Reaction of **10** with **11** under high dilution conditions led to unsymmetrical macrocycle **12** in a yield of 15−20%. Treatment of the protected intermediate **12** with BBr_3 in this instance resulted in simultaneous removal of both ether and amine protective groups (53%). Reaction of the resultant amine derivative **7** with glutaric anhydride led to the formation of carboxylic acid **8** in high yield (85%); this in turn was used to form active ester **9** in 90% yield under standard conditions.

In all cases, formation of the corresponding Tb(III) complexes occurred spontaneously upon heating ligands **6**, **7**, **8**, or **9** in methanol containing pyridine as a base with a solution of Tb(III).

Due to the coexistence of several possible conformers/isomers in solution, it was difficult to characterize these macrotricycles using only NMR spectroscopy. In the case of BH(2,2)IAM (Figure 1, **6**), the deprotected ligand is highly symmetric, and this high symmetry should be reflected in the NMR spectra. The HPLC chromatogram showed only one sharp peak, identified by mass spectroscopy as the desired macrotricyclic ligand. However, the observed NMR (^1H and ^{13}C) spectra in DMSO-d_6 or CD_3OD were difficult to resolve, suggesting the coexistence of several conformers/isomers. Upon changing the solvent to D_2O−NaOD, the ^1H and ^{13}C NMR experiments reveal clearly resolved spectra (Figure 2). This is consistent with the expected high molecular symmetry and suggests that in highly basic solution the phenolic protons are fully deprotonated, destroying the network of intramolecular hydrogen bonding observed in the crystal structure of the precursor protected ligand (*vide infra*). This generates a highly symmetric tetraanion (Figure 2). For the other asymmetric macrotricycles **7**−**9**, NMR characterization was even more challenging. The combination of HPLC with mass spectroscopy and elemental analysis was necessary to characterize these compounds further (see Supporting Information).

X-ray Crystal Structure of Me_4BH(2,2)IAM, 5. X-ray quality crystals of the methyl protected macrotricycle, conforming to space group *C*2/*c*, were obtained as the complex of triethylammonium

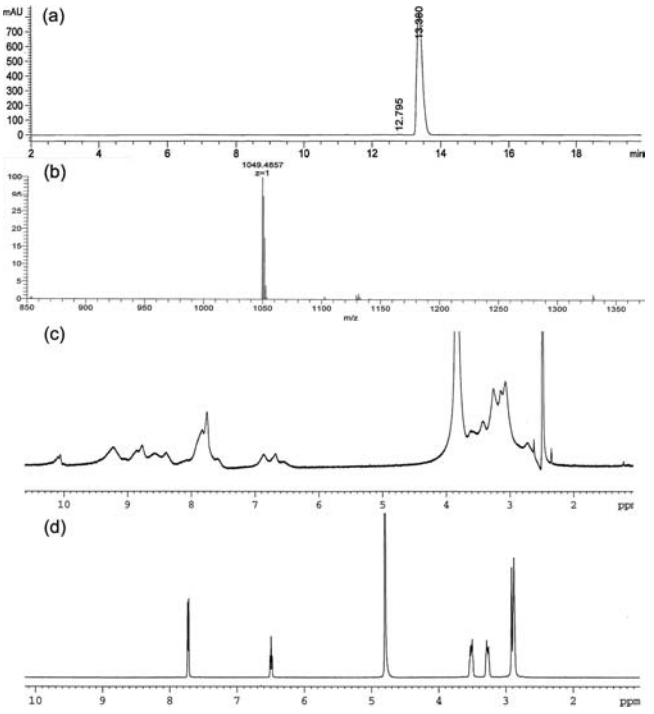

Figure 2. Characterization of BH(2,2)IAM, **6**. (a) Reverse-phase HPLC chromatogram, (b), high resolution mass spectrum, (c) ^{1}H NMR spectrum in DMSO-d_6, and (d) ^{1}H NMR spectrum in D_2O−NaOD. Changing the solvent from DMSO-d_6 to D_2O−NaOD revealed a clearly resolved ^{1}H NMR spectrum.

chloride, $Et_3NH^+[\mathbf{5}(Cl^-)]\cdot H_2O$, in which the protected macrotricycle acts as an amide-based anion receptor. A summary of the full crystallographic data and structural refinement details is in Table 1.

The macrotricycle is a cage composed of two H(2,2) capping moieties and four 2-methoxyisophthalamide units. The bicapped topology of this compound inherently generates a central cavity defined by the two capping units and the four methyl protected chelating units. The lone pairs of the four tertiary amines on the caps are all directed inward, while all four methyl groups are directed outward, with a guest chloride anion filling the cavity of the molecule. The amide protons of each NH group are hydrogen bonded to their respective methoxy oxygen atoms, and this motif of hydrogen bonding results in a nearly planar structure, as is well documented for terephthalamide chelating groups.[22,28] The single chloride anion is bound within the macrotricycle through four amide hydrogen bonds (average distance = 2.912 Å). The four diamido IAM groups adopt an up−down−up−down arrangement with pseudo-S_4 symmetry, as shown in Figure 3.

The four IAM groups are coplanar and are arranged in pairs (C4A−C9A, C4B−C9B, C4C−C9C, and C4D−C9D respectively), each of which is essentially parallel, with dihedral angles of 2.47 (0.11°) and 3.17 (0.13°), respectively. Each of these pairs is offset and $\pi-\pi$ stacking is evident, with the distances of each pair of carbon atoms adjacent to phenolic oxygens being 3.383 (4) and 3.318 (4) Å, respectively. Unlike our previously reported structure of Me_8BH(2,2)CAM,[21] in which the four aromatic rings are parallel to each other, in this case, the two pairs of IAM rings form dihedral angles of ca. 59.4°, as shown in Figure 4.

Table 1. Summary of Crystal Data and Structure Refinement Parameters for 5, Me_4BH(2,2)IAM

identification code	$Et_3NH^+[\mathbf{5}(Cl^-)]\cdot H_2O$	
empirical formula	$C_{62}H_{90}ClN_{13}O_{13}$	
formula weight	1260.92 g·mol^{-1}	
temperature	100(2) K	
wavelength	1.54178 Å	
crystal system, space group	monoclinic, $C2/c$	
unit cell dimensions	a = 39.4197(11) Å	α = 90°
	b = 13.7261(4) Å	β = 122.1540(10)°
	c = 30.1648(9) Å	γ = 90°
volume	13818.1(7) Å^3	
Z, calcd density	8, 1.212 g/cm^3	
absorption coefficient	1.046 mm^{-1}	
F(000)	5392	
crystal size	0.16 × 0.11 × 0.07 mm^3	
θ range for data collection	2.65−68.39°	
limiting indices	$-47 \le h \le 45$, -16	
	$\le k \le 15$, $-36 \le l \le 36$	
reflections collected/unique	59580/12464 [R(int) = 0.0182]	
completeness to θ = 68.39	98.1%	
absorption correction	semiempirical from equivalents	
max. and min transmission	0.9304 and 0.8505	
refinement method	full-matrix least-squares on F^2	
data/restraints/parameters	12464/0/815	
goodness-of-fit on F^2	1.035	
final R indices [$I > 2\sigma(I)$][a]	R_1 = 0.0507, wR_2 = 0.1460	
R indices (all data)	R_1 = 0.0548, wR_2 = 0.1495	
largest diff peak and hole	1.012 and −0.713 e·A^{-3}	

[a] $R_1 = \Sigma(||F_o| - |F_c||)/\Sigma(|F_o|)$; $wR_2 = [\Sigma\{w(F_o^2 - F_c^2)^2/\Sigma\{w(F_o^2)^2\}\}]^{1/2}$.

Each of the four IAM arms of the macrotricycle contain a five-atom hydrogen bonding network between the amide hydrogen protons and the lone pairs on adjacent phenolic oxygen and amine nitrogen atoms (N3···H1AA(N1A)···O2A···H2AA (N2A)···N5; etc.) as shown schematically in Figure 5a. The overall three-dimensional ring arrangement of the structure resulting from these hydrogen bonds is more clearly seen in Figure 5, and the lengths of these hydrogen bond interactions are summarized in Table 2.

Photophysical Properties of Tb(III) Complexes with IAM Ligands and Bioconjugates. The UV−visible absorption spectra of the Tb(III) complexes are summarized in Table 3, and the spectrum of Tb−**6** is shown as an example in Figure 6. Notably, the molar extinction coefficients for Tb−**6** and Tb−**7** are quite similar, albeit slightly lower than those previously reported for Tb−**4**, while that of Tb−**8** is considerably reduced. The reasons for these differences are not readily apparent. However, for the macrotricyclic complexes we note that the trend in the apparent decrease follows the change in the overall charge of the complex under identical conditions of protonation (*e.g.* $[Tb-\mathbf{8}]^{2-}$, $[Tb-\mathbf{6}]^{-}$, $[Tb-\mathbf{7}]^{0}$), which suggests that the presence of a formal negative charge in proximity to the chromophore strongly influences the transition dipole and, hence, oscillator strength of this $n \rightarrow \pi^*$ transition. Coupled with the slightly lower quantum yields (*vide infra*), this decrease in extinction coefficient results in a reduction of *ca.* 20−30% in the overall brightness, which is a product of the quantum yield and extinction coefficient ($\sim\Phi_{total}\varepsilon_{max}$) of the macrotricyclic complexes, compared to the case of the

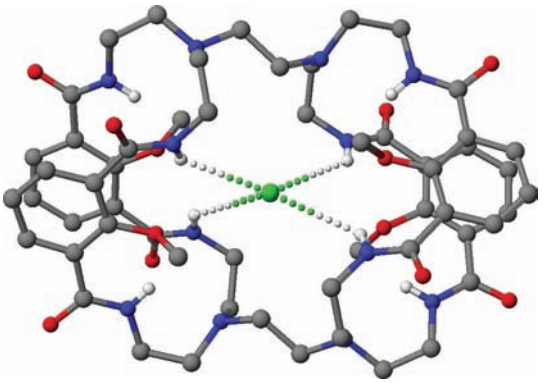

Figure 3. View of the crystal structure of $Me_4BH(2,2)IAM$, **5**, showing the bound chloride anion in close contact with the four amido hydrogens in an alternating "up−down−up−down" arrangement.

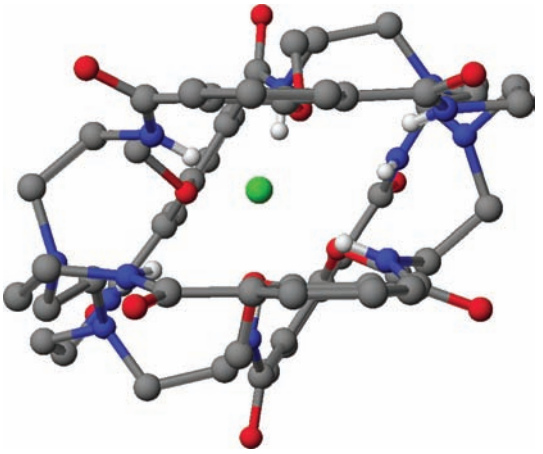

Figure 4. View of the crystal structure of $Me_4BH(2,2)IAM$, **5**, showing the two pairs of IAM groups, which form a dihedral angle of *ca.* 59.4°.

acyclic parent Tb−**4** complex. Nonetheless, these values remain as some of the largest values ever reported for Ln(III) complexes in aqueous solution, and the decreases observed are a small compromise compared to the exceptional kinetic stability imparted by the currently reported complexes.

The normalized emission spectrum of the Tb−**6** complex is also shown in Figure 6, where it is compared to the amine and carboxylate functionalized complexes (Tb−**7** and Tb−**8**) and the spectrum for our previously reported acyclic Tb−**4** complex. Characteristically sharp and structured emission bands from the Tb(III) cation are observed in all cases, which we assign to the $^5D_4 \rightarrow {}^7F_J$ transitions at *ca.* 488 ($J = 6$), 545 ($J = 5$), 580−588 ($J = 4$), 618 ($J = 3$), 650 ($J = 2$), 669 ($J = 1$), and 678−681 nm ($J = 0$), respectively.

Importantly, for the acyclic Tb−**4** complex, we note the intensity of the $^5D_4 \rightarrow {}^7F_6$ transition at *ca.* 490 nm is enhanced compared to the case of the macrotricyclic compounds. Since this transition has known hypersensitivity ($\Delta J = 2$),[1] the decreased intensity of this peak in Tb(III) complexes of the macrotricyclic ligands can be associated with a difference in the coordination geometry at the metal center. We suggest that this change in coordination geometry involves a distortion of the coordinate binding in order to relieve strain within the ensuing macrotricyclic complexes, caused by the bicapped macrotricyclic topology of the chelator.

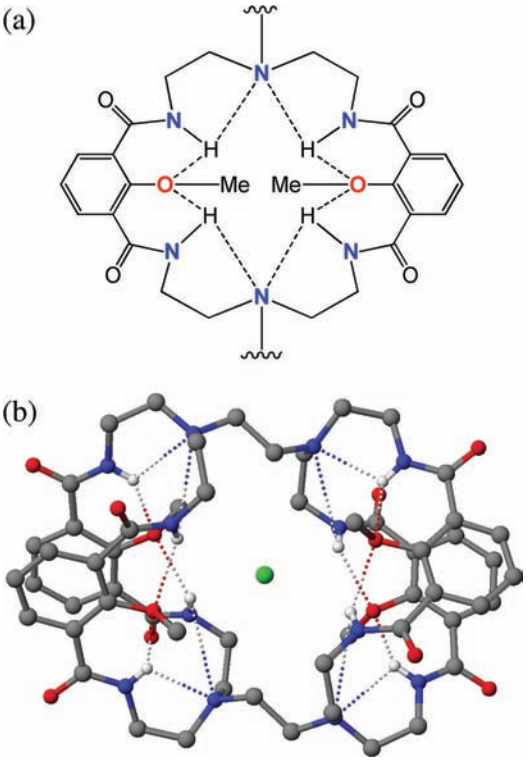

Figure 5. (a) Schematic diagram illustrating the hydrogen bonding motifs within two adjacent IAM chelate branches and (b) view of the crystal structure for $Me_4BH(2,2)IAM$, **5**, illustrating these H-bonding interactions within the whole molecule.

Table 2. Summary of Selected Hydrogen Bond Lengths Observed in Crystals of $Me_4BH(2,2)IAM$,5

D−H···A	distance (Å)	D−H···A	distance (Å)
N1A−H1AA···N3	2.991(3)	N1B − H1BA···N3	2.859(3)
N1A−H1AA···O2A	2.787(2)	N1B− H1BA···O2B	2.677(2)
N2A−H2AA···O2A	2.731(3)	N2B − H2BA···O2B	2.768(2)
N2A−H2AA···N5	2.740(3)	N2B −H2BA···N5	2.962(2)
N1C−H1CA···N4	2.968(2)	N1D−H1DA···N4	2.739(2)
N1−H1CA···O2C	2.784(3)	N1D−H1DA···O2D	2.696(2)
N2C−H2CA···O2C	2.688(3)	N2D−H2DA···O2D	2.791(2)
N2C−H2CA···N6	2.846(3)	N2D−H2DA···N6	2.982(3)

For the family of Tb(III) complexes with the macrotricyclic chelate design, Tb−**6**, Tb−**7**, and Tb−**8** (the latter two with attached linker arms), the emission spectra match closely in all the transitions, with the most intense band attributed to the $^5D_4 \rightarrow {}^7F_5$ transition at *ca.* 545 nm. The overall photophysical properties of the compounds are quite similar, showing that the efficient sensitizing capabilities of the IAM chromophore are retained after incorporation of the macrotricycle structure. The relevant photophysical parameters are summarized in Table 3. Most notably, the overall quantum yield is slightly reduced for the macrotricylic derivatives compared to Tb−**4**, which we can again attribute to a difference in the coordination geometry at the metal center, consistent with the lower intensity of the $^5D_4 \rightarrow {}^7F_6$ transition at *ca.* 490 nm. This difference also influences the observed lifetime, which decreases from 2.60 ± 0.05 ms for

Table 3. Summary of the Photophysical Properties for the Acyclic Tb−4 Complex, the Macrotricyclic Tb−6 Complex, and Its Functionalized Derivatives Tb−7 and Tb−8 ($\lambda_{ex} \sim 340$ nm) in Buffered Aqueous Solution, pH = 7.4

complex	absorption ε_{max} (~340 nm) (M^{-1} cm^{-1})	emission λ_{max} (nm)	Φ_{total}	τ_{H_2O} (pH = 7.4) (ms)	brightness (M^{-1} cm^{-1}) λ_{340nm}
Tb−**4**	26,811	545	0.59	2.60	15,818
Tb−**6**	23,700	545	0.50	2.45	11,850
Tb−**7**	24,300	545	0.52	2.70	12,636
Tb−**8**	20,037	545	0.54	2.67	10,820

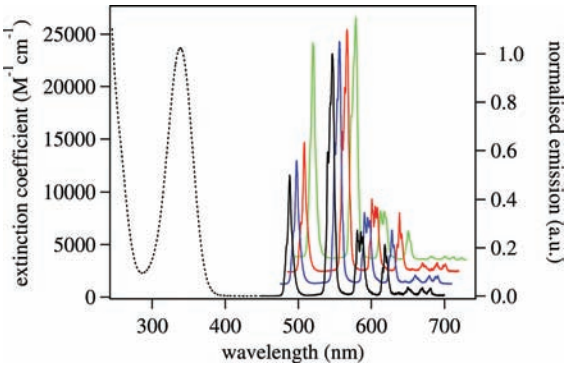

Figure 6. UV−visible absorption spectrum (dotted line) of the Tb−**6** complex (left axis). Emission spectra ($\lambda_{ex} \sim 340$ nm) for the acyclic Tb−**4** complex (green), the macrotricyclic Tb−**6** complex (black), and the functionalized Tb−**7** (red) and Tb−**8** complexes (blue) in buffered aqueous solution, pH 7.4 (right axis). The emission spectra are vertically offset (0.05 au) and horizontally offset (10 nm) for clarity.

Tb−**4** to *ca.* 2.45 ± 0.05 ms for Tb−**6**. However, for Tb−**7** and Tb−**8**, the apparent changes in the radiative decay rates are offset by more effective screening of the complexes from nonradiative quenching by second sphere water molecules for the functionalized macrotricyclic derivatives, due to the steric bulk of the attachment. This results in slight increases of the quantum yields to around 52−54% and recovery of the longer lifetime decays, with almost identical values of 2.70 ± 0.05 and 2.67 ± 0.05 ms observed for Tb−**7** and Tb−**8**, respectively.

The solution stability of Tb−**8** diluted to 5 nM was assessed in various biologically relevant aqueous buffers, including HEPES, tris-buffered saline (TBS), and phosphate buffered saline (PBS) and the biologically relevant competitive additives EDTA and Mg^{2+} (Figure 7). In particular, phosphate anions are known to be a challenging environment for lanthanides due to the highly favored nature of the insoluble $LnPO_4$ salt formation. All conditions tested, except acetic acid, resulted in >80% retention of the luminescence signal beyond 3 days. The notable exception was the low pH environment of 1% acetic acid that can be expected to cause release of the Tb(III) cation following protonation of the chelating isophthalamide subunits, thereby destroying the sensitized metal-centered emission. Nonetheless, even under these conditions, the retention of ~50% of the luminescence signal after 3 days is indicative of the exceptional ability of the macrotricyclic structure to shield the inner coordination environment from the bulk solution.

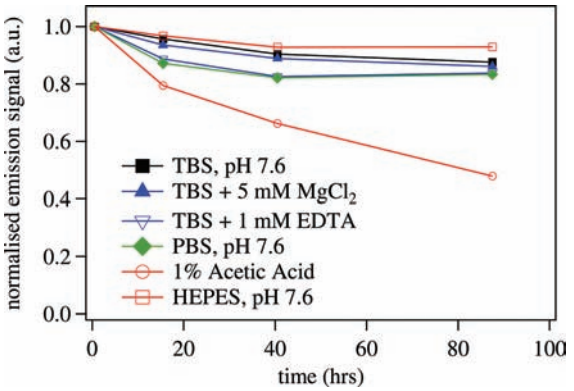

Figure 7. Lanthanide luminescence stability as measured by the luminescence signal intensity at *ca.* 545 nm ($\lambda_{ex} \sim 340$ nm) for various dilute aqueous solutions (5 nM) of Tb−**8** (abbreviations as given in text) at room temperature over time. All solutions also contained 0.05% Tween-20 polysorbate surfactant.

Having demonstrated the exceptional photophysical properties of the macrotricylic Tb(III) complexes, conjugates of Tb−**8** chelate were prepared with several common proteins, including streptavidin (sAv), bovine gamma globulin (BgG), bovine serum albumin (BSA), and mouse immunoglobulin G (IgG). In this case, Tb(III) was added following protein conjugation to ligand **8**, although we point out that protein conjugation using complex Tb−**9** is also feasible (data not shown). The average degree of labeling (DOL) for each molecule was determined using a comparative UV−vis absorption method (see Experimental Section) after metal complexation. The resulting emission spectra of the bioconjugates with sAv, BgG, BSA, and IgG are shown in Figure 8 and are essentially superimposable. Similarly, the emission spectra of the bioconjugates are almost identical to those of the parent macrotricycle, Tb−**6**, and the functionalized Tb−**7** and Tb−**8** complexes, indicating the emissive properties of the Tb(III) complexes are retained upon conjugation to proteins.

To characterize further the spectroscopic behavior of the protein conjugates, the time-resolved decay profiles were measured for each of the samples. In each case, the fit of the experimental data required a biexponential decay function of the form $I_{(t)} = y_0 + A_1 \exp^{(-1/\tau_1)t} + A_2 \exp^{(-1/\tau_2)t}$, with resulting fit parameters as summarized in Table 4. In each case, the major component of the time-resolved luminescence decay signal can be attributed to emission from the Tb−**8** complex, bound to the relevant biomolecule, and the lifetime of this component is essentially unchanged within the experimental error of *ca.* ± 10% in most cases. However, we do note that heavier labeling for the IgG conjugates, in particular, induces a slight decrease in the luminescence lifetime of the Tb−**8** signal (*e.g.* IgG−Tb−**8** (DOL = 2.9; ~2.55 ms) *cf.* IgG−Tb−**8** (DOL = 5.4; ~2.40 ms)), which we can attribute to self-quenching (*e.g.* via cross-relaxation processes), which can often be observed when the local concentration of metal centers is high.[36] This is in contrast to comparable labeling levels achieved with the much smaller protein sAv, which did not exhibit a similar lifetime decrease, even though the average spacing between labeling sites would be expected to be smaller and, therefore, more susceptible to self-quenching. These data suggest that the distribution of labeling sites for IgG may be more suited to cross-relaxation processes than those of streptavidin, although the overall effect is minimal. Similarly, the

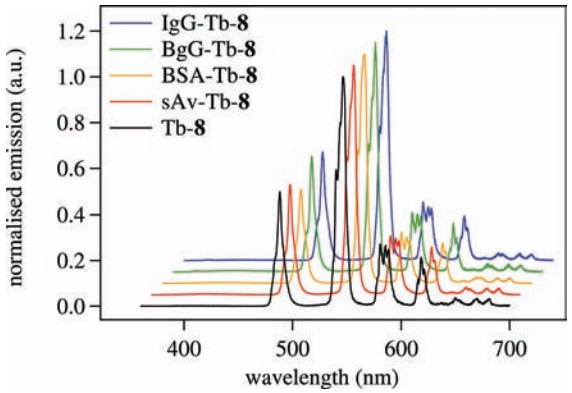

Figure 8. Comparison of the emission spectra ($\lambda_{ex} \sim 340$ nm) for Tb−**8** conjugated to various proteins, including BSA, sAv, IgG, and BgG in buffered aqueous solution, pH 7.4. All conjugates were prepared with periodic monitoring until 3−5 equiv of Tb−**8** was covalently bound. The spectra are vertically offset (0.05 au) and horizontally offset (10 nm) for clarity.

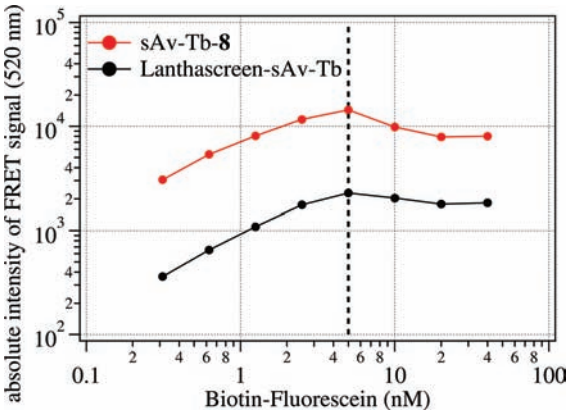

Figure 9. Comparison of FRET signal intensities for various concentrations of biotinylated-fluorescein (Invitrogen) at 520 nm using a 5 nM solution of LanthaScreen-sAv-Tb^{3+} (Invitrogen, DOL = 4.4) or sAv−Tb−**8** (DOL = 4.5) as the long-lived luminescence donor in TBS with 0.05% Tween-20. The dotted line indicates 5 nM biotin-fluorescein yielding an effective 1:1 donor/acceptor ratio.

Table 4. Summary of Photophysical Properties for the Tb−8 Complex after Bioconjugation to sAv, BgG, BSA, and IgG Proteins

complexes	DOL	τ_1 (ms)	A_1 (%)	τ_2 (ms)	A_2 (%)	χ^2
Tb−**8**	N/A	2.67	100			1.06
sAv−Tb−**8**	2.4	2.67	84.4	1.19	15.6	1.03
	4.4	2.69	84.6	1.19	15.4	1.02
IgG−Tb−**8**	2.9	2.55	77.5	1.06	22.5	1.10
	5.4	2.40	64.3	1.08	35.7	1.06
BgG−Tb−**8**	2.5	2.62	86.8	1.02	13.2	1.07
BSA−Tb−**8**	4.4	2.37	63.5	1.04	36.5	1.04

observed lifetime for the BSA conjugate was reduced by ∼10% compared to that of the free Tb−**8** chelate.

The origin of the minor short-lived component observed in the luminescence decays is less clear, although it is most likely related to the use of excess Tb(III) salt during metalation of the labeled proteins, resulting in the formation of a small amount of other emissive Tb(III) protein species. Most importantly, our investigations of the decay lifetime for sAv−Tb−**8** compared to the unconjugated Tb−**8** complex verify that the luminescent properties of Tb−**8** are essentially unaltered following conjugation to streptavidin. Since the local environment of a protein surface conjugation site is often significantly different from that of the free solution and can include hydrophobic regions and areas of high local charge that influence the stability and function of small fluorescent molecules, the lack of significant changes to the photophysical nature of the macrotricycle following protein conjugation is critical.

Lastly, long lifetime lanthanide reporters are particularly suited for use in homogeneous time-resolved Förster resonance energy transfer (TR-FRET) assays. When suitable pairs of compounds are brought into close proximity (<100 nm), resonant coupling can occur, resulting in energy transfer from the excited donor molecule to a ground state acceptor. The excited acceptor molecule can then decay radiatively via the emission of light at its own characteristic wavelength or nonradiatively via vibrational or other quenching mechanisms. Compound Tb−**8** was evaluated as a FRET donor in this way, using a model streptavidin system. Streptavidin covalently labeled with Tb−**8** was incubated with various concentrations of commercially available biotinylated fluorescein. Following excitation of Tb−**8** at 340 nm, the fluorescein emission signal was monitored at 520 nm (10 nm bandpass filter), where emission from the Tb−**8** complex is negligible. Due to the low extinction coefficient of fluorescein at 340 nm (3,500 M^{-1} cm^{-1}), the large effective Stokes shift for excitation of Tb−**8**, and the short lifetime typical of organic fluorophores, there is negligible direct fluorescein signal at 520 nm, resulting in an almost pure TR-FRET signal. Utilizing Tb−**8** as a donor, the intensity of the TR-FRET signal was also compared with that of a commercially available LanthaScreen Streptavidin−Tb^{3+} conjugate (LanthaScreen sAv-Tb^{3+}),[29] with results as summarized in Figure 9. The intensity of the FRET signal roughly track the order of magnitude quantum yield increase of Tb−**8** compared to the LanthaScreen sAv-Tb^{3+} compound.[11] It was also noted that donor/acceptor ratios greater than 1:1 resulted in a net decrease in FRET signal, resulting in a nonlinear response which we attribute to self-quenching of the fluorescein acceptor in the local environment of the sAv protein surface when more than one fluorescein molecule per protein was present.

CONCLUSION

A new octadentate macrotricyclic terbium(III) luminescent chelator, BH(2,2)IAM (**6**), has been developed on the basis of the bicapped H(2,2) topology with four 2-hydroxyisophthalamide (IAM) chelating units. The bicapped H(2,2) topology generates a central cavity predisposed toward Ln(III) binding, leading us to prepare and evaluate derivatives of the corresponding macrotricyclic Tb(III) complex as luminescent labels in TR-FRET-based bioassays. The archetypical complex of Tb(III) with **6** and its functionalized derivatives **7** and **8** exhibit exceptionally high quantum yields ($\Phi_{total} \geq 50\%$), large extinction coefficients ($\geq$20,000 $M^{-1}cm^{-1}$), and long luminescence lifetimes ($\geq$2.45 ms) as compared to other reported compounds. We have also shown that these properties are retained at dilute concentration and display excellent long-term stability, with little change over extended periods of time, even in the presence of competing

ligands such as EDTA or phosphate buffer. Moreover, we have demonstrated that the photophysical properties of the bicapped H(2,2) IAM Tb(III) complex are retained in protein bioconjugates and that the streptavidin conjugate performs favorably as a FRET donor as compared with an existing luminescent Tb(III) system. These compounds therefore establish a new aqueous stability and quantum yield performance standard for long-lifetime lanthanide reporters for use in high throughput screening (HTS) and for diagnostic applications using homogeneous TR-FRET assays.

EXPERIMENTAL SECTION

Materials. All solvents for synthesis were dried using standard methodologies. Thin-layer chromatography (TLC) was performed using precoated Kieselgel 60 F254 plates. Flash chromatography was performed using EM Science Silica Gel 60 (230−400 mesh). NMR spectra were obtained using either Bruker AM-300 or DRX-500 spectrometers operating at 300 (75) MHz and 500 (125) MHz for ^{1}H (or ^{13}C), respectively. ^{1}H (or ^{13}C) chemical shifts are reported in parts per million (ppm) relative to the solvent resonances, taken as δ 7.26 (δ 77.0) and δ 2.49 (δ 39.5) for $CDCl_3$ and $(CD_3)_2SO$, respectively, while coupling constants (J) are reported in hertz (Hz). For the asymmetrically substituted macrotricyclic ligands (**7**, **8**, **9**, and **12**), the observed ^{13}C NMR spectra were very complicated, due to the presence of differing conformers/isomers in solution, and are not reported (see Supporting Information). Analytical HPLC was performed on an Agilent 1200 instrument (Agilent, Santa Clara, CA) equipped with a diode array detector (λ = 254, 280, 313, and 333 nm), a thermostat set at 25 °C, and a Zorbax Eclipse XDB-C18 column (4.6 mm × 150 mm, 5 μm, Agilent, Santa Clara, CA). The mobile phase of a binary gradient (0−40% B/20 min; solvent A, 0.1% TFA; solvent B, ACN for method 1) at a flow rate of 1 mL/min was used for analytical HPLC. Electrospray ionization (ESI) high-resolution mass spectra (HRMS) and elemental analyses were performed at the Microanalytical Facility, College of Chemistry, University of California, Berkeley, CA. Tb(III) complexes reported herein were prepared either by isolation after extended heating in nonaqueous solvent or by mixing the required ligand and metal salt together at room temperature in buffered aqueous solutions. It is not necessary to apply heat to prepare the complexes, but this is a common technique, which was used in some cases. Yields indicate the amount of isolated compounds, and reactions are not optimized. Proteins used for bioconjugation reactions were obtained from either Prozyme (San Leandro, CA), or Biostride, Inc. (Redwood City, CA), and all bioconjugation reactions were performed using well accepted techniques.[30] LanthaScreen Streptavidin−Tb^{3+} was purchased from Invitrogen Inc. (Carlsbad, CA). All other reagents were used as supplied.

Synthesis of Ligands. Detailed syntheses of the necessary starting materials (compounds **10** and **11**, as shown in Scheme 1), *N*,*N*′,*N*″,*N*‴-[1,2-ethanediylbis(nitrilodi-2,1-ethanediyl)]tetrakis[2-methoxy-3-[(2-thioxo-3-thiazolidinyl)carbonyl]]-*N*,*N*′,*N*″,*N*‴-[1,2-ethanediylbis-(nitrilodi-2,1-ethanediyl)]tetrakis[2-methoxy-3-[(2-thioxo-3-thiazolidinyl)carbonyl]]benzamide [H(2,2)IAMtetrathiazolide, (**10**)] and (*S*)-*tert*-butyl-5-amino-6-((2-aminoethyl)(2-(bis(2-aminoethyl)amino)ethyl)-amino)hexylcarbamate [BocLys-H(2,2)amine (**11**)], have been previously reported.[16,23]

*Me_4BH(2,2)IAM (**5**).* This protected ligand was synthesized under high dilution conditions. Compound **10** (1.35 g, 1 mmol) and Penten[37] (0.24 g, 1 mmol) were dissolved in 500 mL of CH_2Cl_2 separately. The two solutions were added to a stirred 3.5 L CH_2Cl_2 solution containing 2 mL of Et_3N in a 5 L round-bottom flask simultaneously over a period of 7 days. The addition was controlled to maintain a pale yellow color in the reaction flask in order to minimize polymeric byproduct. The reaction mixture was stirred an additional 8 h after all the reactants had been added. The reaction mixture was evaporated to dryness to leave a light yellow oily material. The appropriate fractions of a gradient flash column (3−7% MeOH in CH_2Cl_2) were evaporated to dryness to give the product as a white foam. Yield: 0.57 g (52%). MS (ESIHR) for $C_{56}H_{73}N_{12}O_{12}$ [MH^+], calcd (found) *m*/*z*: 1105.5465 (1105.5492). ^{1}H NMR (500 MHz, $CDCl_3$, 25 °C) δ: 2.57 (br s, 8H, CH_2), 2.82 (br t, 8H, CH_2), 2.93 (m, 8H, CH_2), 3.47 (m, 12H, CH_2), 3.65 (s, br 16H, CH_3), 5.29 (s, 16H, CH_2), 7.07 (t, 4H, *J* = 7.5, ArH), 7.53 (s, br, 8H, NH), 7.75 (d, 8H, *J* = 7.5, ArH). ^{13}C NMR (125 MHz, $CDCl_3$, 25 °C) δ: 37.6, 51.4, 52.2, 62.8, 124.6, 127.0, 133.6, 155.1, 165.0. Crystals of methyl protected ligand **5** suitable for X-ray diffraction were grown by slow diffusion of *tert*-butyl methyl ether into a wet methanol solution of **5** in the presence of excess triethylamine HCl salt.

*BH(2,2)IAM (**6**).* Compound **5** (0.55 g, 0.5 mmol) was dissolved in 30 mL of CH_2Cl_2 in a Schlenk flask with a Teflon stopcock. Under a flow of N_2, the solution was cooled to −10 °C before 2.0 mL of BBr_3 was injected. The slurry was stirred for 4 days before removing the excess BBr_3 and CH_2Cl_2 in vacuo. The remaining light yellow solid was dissolved in MeOH (50 mL) with cooling. The MeOH solution was heated at reflux overnight and poured into H_2O (100 mL). The resulting solution was boiled until the volume was reduced to *ca.* 50 mL and then cooled, affording the product as a white solid, which was collected by filtration and oven-dried. Yield: 550 mg (73%). Calcd %. (Found %) for $C_{54}H_{68}N_{12}O_{12}\cdot 4HBr\cdot 5.75H_2O$ (1504.5 g mol^{-1}): C, 43.11 (43.44); H, 5.59 (5.55); N, 11.17 (10.78). MS (ESIHR) for $C_{52}H_{65}N_{12}O_{12}$ [MH^+], calcd (found) *m*/*z*: 1049.4839 (1049.4857). ^{1}H NMR (500 MHz, D_2O−NaOD, 25 °C) δ 2.88 (br s, 16H, CH_2), 2.92 (s, 8H, CH_2), 3.28 (m, 8H, CH_2), 3.52 (m, 8H, CH_2), 6.49 (t, 4H, *J* = 7.5, ArH), 7.73 (dd, 8H, *J* = 7.5, ArH). ^{13}C NMR (75 MHz, D_2O−NaOD, 25 °C) δ: 37.4, 51.3, 52.4, 112.3, 120.7, 134.3, 170.2, 170.4.

*Me_4BocLysBH(2,2)IAM (**12**).* This compound was prepared by the high dilution procedure as for **5** ,except BocLysH(2,2)amine (**11**) (0.40 g, 1 mmol, 1 equiv) with 1.05 mL of *N*,*N*-diisopropylethylamine (DIEA) (6 mmol, 6 equiv) and 3 mL of isopropyl alcohol (IPA) were used instead of Penten. The cyclization reaction is slower than that of **5**, so the addition of reactants took a period of 8−10 days. The addition rates were adjusted to about 50−60 mL per 24 h for each reactant, yielding a pale yellow color solution in the reaction flask. It is necessary to maintain the high dilution conditions in order to minimize polymeric byproduct. After all the reactants were consumed, the reaction mixture was stirred an additional 8 h. TLC on silica gel revealed the reaction mixture to be a complicated mixture. The reaction mixture was passed through a flash silica column (200 g) to remove most of the polymeric byproduct, and the raw product was then separated by gradient flash chromatography (2−10% MeOH + 0.5% DIEA in CH_2Cl_2). Further purification of the raw product was then performed by sequential basic alumina column and gradient flash silica column chromatography (3−7% MeOH in CH_2Cl_2) to afford the desired product as a white foam. The typical yield of the desired macrotricycle was about 15−20%. MS (ESIHR) for $C_{65}H_{90}N_{13}O_{14}$ [MH^+], calcd (found) *m*/*z*: 1276.6725 (1276.6736). ^{1}H NMR (500 MHz, $CDCl_3$, 25 °C): δ 1.24−1.55 (m, 15H, Boc CH_3 + Lys CH_2), 2.52−2.95 (m, br, 24H, NCH_2), 3.21−3.62 (m, br, 17H, $NHCH_2$), 3.65−3.7 (m, 12H, CH_3), 6.78 (s br, 1H, BocNH), 6.90−7.15 (m, 8H, ArH), 7.50−7.90 (m, 16H + 8H, ArH + amide H).

*LysBH(2,2)IAM (**7**).* Compound **12** (0.22 g, 0.17 mmol) was dissolved in 20 mL of degassed CH_2Cl_2 in a Schlenk flask with a Teflon stopcock. Under a flow of N_2, the solution was cooled to −10 °C before 1 mL of BBr_3 was injected. The slurry was stirred for 6 days before pumping off the excess of BBr_3 and CH_2Cl_2. The remaining light yellow solid was dissolved in MeOH (100 mL) with cooling [dry ice/isopropanol (IPA) bath]. The MeOH solution was gently refluxed with stirring and left uncapped to allow the release of volatile boron compounds for 6−10 h in an efficient fume hood and then evaporated to dryness. The residue was redissolved in MeOH (20 mL) and diluted into milli-Q H_2O

(50 mL). The mixed solution was then boiled gently until the volume was reduced to about 1 mL, allowing the precipitation of the HBr salt of the macrotricycle as a white solid upon cooling, which was collected by centrifugation and vacuum-dried at 40 °C. Yield: 150 mg (53%). The purity of compound **7** was further characterized by HPLC and MS. MS (ESIHR) for $C_{56}H_{74}N_{13}O_{12}^{+}$ [MH^+], calcd (found) m/z: 1120.5574 (1120.5596). Anal. Calcd % (Found %) for $C_{56}H_{73}N_{13}O_{12}\cdot 5HBr\cdot 8H_2O$ (1668.95 g·mol^{-1}): C, 40.30 (40.29); H, 5.68 (5.68); N, 10.91 (10.65). ^{1}H NMR (500 MHz, $D_2O-K_2CO_3$, 25 °C): δ 1.29−1.90 (m, 6H, CH_2), 2.40−3.10 (m, br, 28H, NCH_2), 3.21−3.62 (m, br, 10H, $NHCH_2$), 3.65−4.2 (m, 3H, CH + CH_2), 6.30−6.60 (m, 4H, ArH), 7.50−7.80 (m, 8H, ArH).

*GlutarLysBH(2,2)IAM (**8**).* LysBH(2,2)IAM (**7**) (167 mg, 0.1 mmol) and diisopropylethylamine [DIEA (0.5 mL)] were dissolved in 5 mL of dry DMF. After it was stirred at room temperature for 4 h, the reaction mixture was evaporated to dryness. The remaining light yellow solid was dissolved in dry DMF (5 mL) under N_2, and glutaric anhydride (12 mg, 1.05 equiv) was added with stirring. After it was stirred for 2 h, an additional portion of glutaric anhydride (3 mg, 0.26 equiv) was added to ensure the reaction had gone to completion, as monitored by HPLC. The reaction mixture was then added to a stirred solution of IPA dropwise, and a precipitate formed immediately. Three drops of concentrated HBr was added to the stirring slurry (pH ∼ 4) to promote the precipitation of the product as the HBr salt. The precipitate was separated by centrifugation and resuspended in dry IPA to wash away the impurities. The product was collected by centrifugation and vacuum-dried. Yield: 134 mg (85%). The purity of compound **8** was further characterized by HPLC and MS.MS (ESIHR) for $C_{61}H_{80}N_{13}O_{15}^{+}$ [MH^+], calcd (found) m/z: 1234.5892 (1234.5906). Anal. Calcd % (Found %) for $C_{61}H_{79}N_{13}O_{12}\cdot 3HBr\cdot 5.5H_2O$ (1576.18 g·mol^{-1}): C, 40.30 (40.29); H, 5.68 (5.68); N, 10.91 (10.65). ^{1}H NMR (500 MHz, $D_2O-K_2CO_3$, 25 °C): δ 1.10−1.40 (m, 6H, CH_2); 1.60−1.70 (m, 2H, CH_2); 1.75−2.45 (m, 6H, CH_2); 2.55−3.15 (m, 26H, CH_2); 3.15−4.15 (m, 13H, CH_2); 6.25−6.60 (m, 4H, ArH); 7.50−8.00 (m, 8H, ArH).

*GlutLysBH(2,2)IAM-NHS (**9**).* GlutLysBH(2,2)IAM (**8**) (80 mg, 0.051 mmol, 1 equiv) and excess NHS (17.5 mg, 3 equiv) were dissolved in dry DMF (5 mL). The mixture was evaporated to dryness after stirring for 2 h. To the dry DMF (5 mL) solution of the residue was added 1,3-diisopropylcarbodiimide (DIC, 0.08 mL, 1 equiv) under N_2. The reaction process was monitored with HPLC after stirring for 2 h, and additional portions (0.025 mL each) of DIC were added to ensure the completion of the reaction. The reaction mixture was then added dropwise to a stirring dry ethyl ether solution to precipitate the product, and the stirring slurry was adjusted to be slightly acidic (pH ∼ 3) with one drop of concentrated HBr solution. The precipitate was collected by centrifugation and washed thoroughly with IPA twice, dried under vacuum (0.1 mmHg) for at least 8 h, and stored in a desiccator at 0−4 °C. Yield: 76 mg (0.0457 mmol, 90%). The purity of compound **9** was further characterized by HPLC and MS. MS (ESIHR) for $C_{65}H_{83}N_{14}O_{17}^{+}$ [MH^+], calcd (found) m/z: 1331.6055 (1331.6083). Anal. Calcd % (Found %) for $C_{65}H_{82}N_{14}O_{17}\cdot 4HBr\cdot 5H_2O$ (1745.15 g·mol^{-1}): C, 44.74 (45.05); H, 5.54 (5.49); N, 11.24 (10.88). ^{1}H NMR (500 MHz, DMSO-d_6, 25 °C): δ 1.10−1.55 (m, br, 6H, CH_2); 1.60−1.90 (m, br, 2H, CH_2); 1.95−2.25 (m, br, 2H, CH_2); 2.55−2.75 (m, br, 4H, CH_2); 2.90−3.80 (m, br, 24H, CH_2), 3.80−4.50 (m, 19H, CH_2); 6.10−7.10 (m, 4H, ArH); 7.30−8.15 (m, 8H, ArH); 8.20−10.2 (m, 9H, amideH).

Synthesis of Tb(III) Complexes. *Tb−BH(2,2)IAM (Tb−**6**).* To a solution of BH(2,2)IAM HBr salt hydrate (**6**) (15.8 mg, 11 umol) in MeOH (15 mL) was added a solution of Tb(III) chloride hexahydrate (99.99%, 3.7 mg, 10 umol) in MeOH (2 mL) with stirring. The mixture was heated to gentle reflux, and a few drops of pyridine were added. After the solution was heated at 60 °C for 2 h, the solution volume was reduced to about 10% and the complex was precipitated as a white solid. It was filtered, washed twice with cold MeOH (2 × 5 mL), and vacuum-dried. Yield: 12.1 mg (83%). MS (ESIHR) for $TbC_{52}H_{62}N_{12}O_{12}^{+}$ [MH^+], calcd (found) m/z: 1205.3859 (1205.3854). Anal. Calcd % (Found %) for $TbC_{52}H_{62}N_{12}O_{12}\cdot 2HBr\cdot 5H_2O$ (1456.24 g·mol^{-1}): C, 42.89 (43.11); H, 5.05 (5.49); N, 11.54 (11.41).

*Tb−LysBH(2,2)IAM (Tb−**7**).* This complex was prepared in a similar manner as Tb−**6**, except LysBH(2,2)IAM (**7**) was used instead of **6**. Yield: 85%. MS (ESIHR) for $TbC_{56}H_{71}N_{13}O_{12}^{+}$ [MH^+], calcd (found) m/z: 1276.4593 (1276.4561). Anal. Calcd % (Found %) for $TbC_{56}H_{70}N_{13}O_{12}\cdot 3HBr\cdot 2.5H_2O$ (1625.04 g·mol^{-1}): C, 43.68 (43.61); H, 5.40 (5.25); N, 11.27 (11.26).

*Tb−GlutLysBH(2,2)IAM (Tb−**8**).* This complex was prepared in a similar manner as Tb−**6**, except GlutLysBH(2,2)IAM (**8**) was used instead of **6**. Yield: 81%. MS (ESIHR) for $TbC_{61}H_{77}N_{13}O_{15}^{+}$ [MH^+], calcd (found) m/z: 1390.4910 (1390.4925). Anal. Calcd % (Found %) for $TbC_{61}H_{76}N_{13}O_{15}\cdot 2HBr\cdot 10H_2O$ (1732.63 g·mol^{-1}): C, 42.30 (42.22); H, 5.70 (5.80); N, 10.69 (10.50).

*Tb−GlutLysBH(2,2)IAMNHS (Tb−**9**).* This complex was prepared in a similar manner as Tb−**6**, except GlutLysBH(2,2)IAMNHS (**9**) was used instead of **6**. Yield: 82%. MS (ESIHR) for $TbC_{65}H_{80}N_{14}O_{17}^{+}$ [MH^+], calcd (found) m/z: 1487.5074 (1487.5068). Anal. Calcd % (Found %) for $TbC_{65}H_{82}N_{14}O_{17}\cdot 4HBr\cdot 5H_2O$ (1745.15 g·mol^{-1}): C, 44.74 (45.05); H, 5.54 (5.49); N, 11.24 (10.88).

Photophysical Measurements. UV/visible spectra were recorded on a Varian Cary 300 double beam spectrometer using quartz cells of 1 cm path length. Emission spectra were measured using a HORIBA Jobin Yvon Fluorolog-3 spectrofluorometer equipped with an IBH TBX-04-D detector. Spectra were reference corrected for both excitation light source variation (lamp and grating) and emission spectral response (detector and grating). Luminescence lifetimes were determined with a HORIBA Jobin Yvon IBH FluoroLog-3 spectrofluorimeter, adapted for time-resolved measurements using the MCS technique. A submicrosecond xenon flash lamp (Jobin Yvon, 5000XeF) was used as the light source, coupled to a double grating excitation monochromator for spectral selection. The input pulse energy (100 nF discharge capacitance) was *ca.* 50 mJ, yielding an optical pulse duration of less than 300 ns at fwhm. A thermoelectrically cooled single photon detection module (HORIBA Jobin Yvon IBH, TBX-04-D) incorporating a fast rise time PMT, a wide bandwidth preamplifier, and a picosecond constant fraction discriminator was used as the detector. Signals were acquired using an IBH DataStation Hub photon counting module, and data analysis was performed using the commercially available DAS 6 decay analysis software package from HORIBA Jobin Yvon IBH. Goodness of fit was assessed by minimizing the reduced chi squared function, χ^2, and a visual inspection of the weighted residuals. Each trace contained at least 10,000 points, and the reported lifetime values result from at least three independent measurements.

Quantum yield measurements were determined by the optically dilute method using the following equation:

$$\frac{\Phi_x}{\Phi_r} = \left[\frac{A_r(\lambda_r)}{A_x(\lambda_x)}\right]\left[\frac{I(\lambda_r)}{I(\lambda_x)}\right]\left[\frac{{\eta_x}^2}{{\eta_r}^2}\right]\left[\frac{D_x}{D_r}\right]$$

where A is the absorbance at the excitation wavelength (λ), I is the intensity of the excitation light at the same wavelength, η is the refractive index, and D is the integrated luminescence intensity. The subscripts "x" and "r" refer to the sample and reference, respectively. Quinine sulfate in 1.0 N sulfuric acid (Φ_r = 0.546) was used as a reference standard.[31] All photophysical measurements were performed with complexes made in situ in either Hepes or Tris buffer, unless otherwise stated, at pH 7.4.

Structure Determination. A single crystal of compound **5** suitable for X-ray crystallography (0.16 mm × 0.11 mm × 0.07 mm) was coated in Paratone-N oil and mounted on a Cryo loop. The loop was transferred to a MicroSTAR-H X8 diffractometer equipped with a CCD

area detector,[32] centered in the beam, and cooled with an Oxford Cryostream 700 LT device. Preliminary orientation matrices and cell constants were determined by collection of three sets of 40, 5 s frames, followed by spot integration and least-squares refinement. COSMO was used to determine an appropriate data collection strategy, and the raw data were integrated using SAINT.[33] Cell dimensions reported were calculated from all reflections with $I > 10\,\sigma$. The data were corrected for Lorentz and polarization effects; no correction for crystal decay was applied. Data were analyzed for agreement and possible absorption using XPREP.[34] An absorption correction based on comparison of redundant and equivalent reflections was applied using SADABS.[35] The structure was solved by sira 2004[36] and refined on F^2 using SHELXL-97.[37] Thermal parameters for all non-hydrogen atoms were refined anisotropically. One terminal methyl group of triethylamine is disordered between two positions. The structure diagrams were created using the ORTEP-3 software package.[38] In the lattice, there are a few unresolved disordered methanol and water molecules which were treated with the SQUEEZE routine included in PLATON.[39] The final refinement by this approach provided significantly better residuals.

Protein Conjugation, Labeling, and Comparison Studies. GlutarLysBH(2,2)IAM (**8**) was dissolved with 5−6 equiv of sulfo-*N*-hydroxysuccinimide (sNHS, Pierce) and 7−8 equiv of 1-ethyl-3-(3-dimethylaminopropyl) carbodiimide (EDC, Pierce) to a final concentration of 20−40 mM (**8**) in dry DMF, and then the resulting solution was stirred at RT for at least 2 h. The GlutarLysBH(2,2)IAM-sNHS forming in situ was then slowly added to protein solutions ranging from 28−740 uM that were previously buffer exchanged into 100 mM Na_2CO_3 buffer (pH 9). Mouse IgG (28 uM), bovine gamma globulin (BgG, 200 uM), streptavidin (sAv, 92−105 μM), and bovine serum albumin (BSA, 740 μM) solutions were allowed to stir at room temperature, following reagent addition, and were monitored for conjugation progress periodically. The protein conjugates were then separated from unreacted compounds via buffer exchange into 0.1 M Tris, pH 7.6, using a Sephadex G50 column.[40−42] $TbCl_3 \cdot 6H_2O$ (~2.5 equiv) dissolved in sodium citrate (pH = 5.0) was then added to the conjugate while stirring to form the metal complex over 5−10 min. The degree of labeling (DOL) was determined from absorbance data collected at 280 and 339 nm using an extinction coefficient of ~26,000 M^{-1} cm^{-1} for the macrotricyclic Tb(III) complex, and molecular weights of 150,000 $g \cdot mol^{-1}$ for BgG and IgG, 55,000 $g \cdot mol^{-1}$ for sAv and 66,000 $g \cdot mol^{-1}$ for BSA. A correction of the form $OD_{280corr} = (OD_{280raw} - 0.11OD_{339})$ was made to the raw 280 nm absorbance data to remove the component attributable to the macrotricyclic Tb(III) complex. The labeling ratios of the conjugates were determined to be 2.9 and 5.4 complexes per IgG molecule, 4.4 and 2.4 complexes per sAv molecule, 2.5 complexes per BgG molecule, and 4.4 complexes per BSA molecule.

For comparison studies, LanthaScreen streptavidin conjugate (Invitrogen, Carlsbad, CA) or Tb−**8**−sAv was mixed with biotin−fluorescein (Invitrogen, Carlsbad, CA) to final concentrations of 5 nM sAv and 0.3−40 nM biotin−fluorescein. Readings were conducted in black, 384-well plates with a Perkin-Elmer Envision 2100 reader set for 50 μs delay, 900 μs integration time, and 100 flashes, equipped with a 340 nm excitation filter (60 nm bandpass) and a 520 nm emission filter (10 nm bandpass).

■ ASSOCIATED CONTENT

Supporting Information. HPLC chromatograms, ^1H and ^{13}C NMR spectra, and high resolution mass spectra of the synthesized ligands. X-ray crystallographic information files (CIF) for compound **5**, the protected macrotricyclic ligand Me_4BH(2,2)IAM. This material is available free of charge via the Internet at http://pubs.acs.org.

■ AUTHOR INFORMATION

Corresponding Author
raymond@socrates.berkeley.edu

■ ACKNOWLEDGMENT

Early stages of the ligand synthesis were supported by the NIH (Grants AI11744 and HL69832), and several postdoctoral fellows were supported by individual fellowships from various sources. The lanthanide luminescence project is supported by the Director, Office of Science, Office of Basic Energy Sciences, and the Division of Chemical Sciences, Geosciences, and Biosciences of the U.S. Department of Energy at LBNL under Contract No. DE-AC02-05CH11231. We thank Marcel R. Pirio for early synthetic contributions and Henry K. Tom for helpful discussions; we thank Dr. DiPasquale for assistance with the X-ray structure determinations.

■ REFERENCES

(1) Bünzli, J.-C. G. Luminescent Probes. In *Lanthanide Probes in Life, Chemical and Earth Sciences: Theory and Practice*; Bünzli, J.-C. G., Choppin, G. R., Eds.; Elsevier: Amsterdam, 1989; pp 219−293.
(2) Hemmila, I.; Laitala, V. *J. Fluoresc.* **2005**, *15*, 529–542.
(3) Charbonniere, L. J.; Hildebrandt, N.; Ziessel, R. F.; Loehmannsroeben, H.-G. *J. Am. Chem. Soc.* **2006**, *128*, 12800–12809.
(4) Hemmila, I. *J. Alloys Compd.* **1995**, *225*, 480–485.
(5) Bünzli, J.-C.; Piguet, C. *Chem. Soc. Rev.* **2005**, *34*, 1048–1077.
(6) Jeff, G.; Ge, P.; Selvin, P. R. *Rev. Fluoresc.* **2005**, *2*, 399–431and references therein.
(7) Lehn, J. M.; Mathis, G.; Alpha, B.; Deschenaux, R.; Jolu, E. *Eur. Pat. Appl.* 1989, EP 321353 A1 19890621.
(8) Alpha, B.; Ballardini, R.; Balzani, V.; Lehn, J.-M.; Perathoner, S.; Sabbatini, N. *Photochem. Photobiol.* **1990**, *52*, 299–306.
(9) Prat, O.; Lopez, E.; Mathis, G. *Anal. Biochem.* **1991**, *195*, 283–289.
(10) Bazin, H.; Trinquet, E.; Mathis, G. *Rev. Mol. Biotechnol.* **2002**, *82*, 233–250.
(11) Cisbio Products: HTRF Cryptate Labeling Kit Homepage. http://www.htrf.com/products/labeling/labeling_kit. (accessed Sept 29, 2011).
(12) Xiao, M.; Selvin, P. R. *J. Am. Chem. Soc.* **2001**, *123*, 7067–7073.
(13) Brunet, E.; Juanes, O.; Sedano, R.; Rodriguez-Ubis, J. C. *Photobiol. Sci.* **2002**, *1*, 613–618.
(14) Bourdolle, A.; Allali, M.; Mulatier, J.-C.; Guennic, B. L.; Zwier, J. M.; Baldeck, P. L.; Bünzli, J.-C. G.; Andraud, C.; Lamarque, L.; Maury, O. *Inorg. Chem.* **2011**, *50*, 4987–4999.
(15) Alpha, B.; Balzani, V.; Lehn, J. M.; Perathoner, S.; Sabbatini, N. *Angew. Chem., Int. Ed. Engl.* **1987**, *26*, 1266.
(16) Petoud, S.; Cohen, S. M.; Bunzli, J.-C.; Raymond, K. *J. Am. Chem. Soc.* **2003**, *125*, 13324–13325.
(17) Petoud, S.; Muller, G.; Moore, E. G.; Xu, J.; Sokolnicki, J.; Riehl, J. P.; Le, U. N.; Cohen, S. M.; Raymond, K. N. *J. Am. Chem. Soc.* **2007**, *129*, 77–83.
(18) Seitz, M.; Moore, E. G.; Ingram, A. J.; Muller, G.; Raymond, K. N. *J. Am. Chem. Soc.* **2007**, *129*, 15468–15470.
(19) Raymond, K. N.; Petoud, S.; Cohen, S. M.; Xu, J. U.S. Patent 6406297 B1, 2002; U.S. Patent 6515113 B2, 2003.
(20) Samuel, A. P. S.; Moore, E. G.; Melchior, M.; Xu, J.; Raymond, K. N. *Inorg. Chem.* **2008**, *47*, 7535.
(21) Trinquet, E.; Gregor, N.; Degorce, F.; Tardieu, J.-L.; Seguin, P. In *Introduction of a New TR-FRET Terbium Cryptate* (Poster 11023), Society for Biomolecular Science, Annual Conference and Exhibition, St. Louis, MO, April 6−10, 2008 (see also CisBio HTRF Resource Library Homepage http://www.htrf.com/resources/details/?tid=0&rid=374 (accessed Sept 29, 2011)).
(22) Xu, J.; Stack, T. D. P.; Raymond, K. N. *Inorg. Chem.* **1992**, *31* (24), 4903–5.

(23) Moore, E. G.; Xu, J.; Jocher, C. J.; Corneillie, T. M.; Raymond, K. N. *Inorg. Chem.* **2010**, *49* (21), 9928–9939.
(24) Arano, Y.; Uezono, T.; Akizawa, H.; Ono, M.; Wakisaka, K.; Nakayama, M.; Sakahara, H.; Konishi, J.; Yokoyama, A. *J. Med. Chem.* **1996**, *39*, 3451–3460.
(25) Maisano, F.; Gozzini, L.; De Haen, C. *Bioconjugate Chem.* **1992**, *3*, 212–217.
(26) Reilly, R.; Lee, N.; Houle, S.; Law, J.; Marks, A. *Appl. Radiat. Isot.* **1992**, *43*, 961–967.
(27) Mukkala, V. M.; Sund, C.; Kwiatkowski, M. U.S. Patent 5,216,134, 1993; *Chem. Abstr.* 1993, *119*, 244992.
(28) Garrett, T. M.; Cass, M.; Raymond, K. N. *J. Coord. Chem.* **1992**, *25*, 241–253.
(29) Invitrogen Inc. Products LanthaScreen Tb-Streptavidin Homepage. http://products.invitrogen.com/ivgn/product/PV3966 (accessed Sept 29, 2011).
(30) Hermanson, G. T. *Bioconjugate Techniques*, 2nd ed.; Academic Press: San Diego, 1996; pp 173−176.
(31) Crosby, G. A.; Damas, J. N. *J. Phys. Chem.* **1971**, *75*, 991–1024.
(32) *SMART: Area-Detector Software Package*; Bruker Analytical X-ray Systems, Inc.: Madison, WI, 2001−2003.
(33) *SAINT: SAX Area-Detector Integration Program*, V6.40; Bruker Analytical X-ray Systems, Inc.: Madison, WI, 2003.
(34) *XPREP*; Bruker Analytical X-ray Systems, Inc.: Madison, WI, 2003.
(35) *SADABS: Bruker-Nonius Area Detector Scaling and Absorption*, V2.05; Bruker Analytical X-ray Systems, Inc.: Madison, WI, 2003.
(36) Burla, M. C.; Caliandro, R.; Camalli, M.; Carrozzini, B.; Cascarano, G. L.; De Caro, L.; Giacovazzo, C.; Polidori, G.; Spagna, R. *J. Appl. Crystallogr.* **2005**, *38*, 381–388.
(37) Sheldrick, G. *SHELX-97 Program for Crystal Structure Solution*; Institüt für Anorganische Chemie der Universität: Gottingen, Germany, 1997. Sheldrick, G. *SHELX-97 Program for Crystal Structure Refinement*; Institüt für Anorganische Chemie der Universität: Gottingen, Germany, 1997.
(38) Farrugia, L. J. *J. Appl. Crystallogr.* **1997**, *30*, 565.
(39) Spek, A. L. *PLATON—A Multipurpose Crystallographic Tool*; Utrecht University: Utrecht, The Netherlands, 2007.
(40) Wagnont, B. K.; Jackels, S. C. *Inorg. Chem.* **1989**, *28*, 1923–1927.
(41) Penefsky, H. S. *Methods Enzymol.* **1979**, *56*, 527–530.
(42) Sohn, K.-S.; Choi, Y. Y.; Kim, K. H.; Choi, S. Y.; Park, H. D. *J. Mater. Sci.: Mater. Electron.* **2001**, *12*, 179–186.